Effects of Terrain Morphology, Sampling Density, and Interpolation Methods on Grid DEM Accuracy

Fernando J. Aguilar, Francisco Agüera, Manuel A. Aguilar, and Fernando Carvajal

Abstract

This paper explores the effects of terrain morphology, sampling density, and interpolation methods for scattered sample data on the accuracy of interpolated heights in grid Digital Elevation Models (DEM). Sampled data were collected with a 2 by 2 meters sampling interval from seven different morphologies, applying digital photogrammetric methods to large scale aerial stereo imagery (1:5000). The experimental design was outlined using a factorial scheme, and an analysis of variance was carried out. This analysis yielded the following main conclusions: DEM accuracy (RMSE) is affected significantly by the variables studied in this paper according to "morphology > sampling density > interpolation" method. Multiquadric Radial Basis Function (RBF) was rated as the best interpolation method, although Multilog RBF performed similarly for most morphologies. The rest of RBF interpolants tested (Natural Cubic Splines, Inverse Multiquadric, and Thin Plate Splines) showed numerical instability working with low smoothing factors. Inverse Distance Weighted interpolant performed worse than RBF Multiquadric or RBF Multilog. In addition, it is found that the relationship between the RMSE and the sampling density N is adjusted to a decreasing potential function that may be expressed as $RMSE/Sdz = 0.1906(N/M)^{-0.5684}$ ($R^2 = 0.8578$), *being Sdz the standard deviation of the heights of the M check points used for accuracy estimation, and N the number of sampling points used for creating the DEM. The results obtained in this study allow us to observe the possibility of establishing empirical relationships between the RMSE expected in the interpolation of a Grid DEM and such variables as terrain ruggedness, sampling density, and the interpolation method, among others that could be added. Therefore, it would be possible to establish a priori the optimum grid size required to generate or storage a DEM of a particular accuracy, with the economy in computing time and file size that this would signify for the digital flow of the mapping information.*

Introduction

A Digital Elevation Model (DEM) is a digital and mathematical representation of an existing or virtual object and its environment. As defined by the U.S. Geological Survey, a grid DEM is the digital cartographic representation of the elevation of the land at regularly spaced intervals in *x* and *y* directions, using *z*-values referenced to a common vertical datum. Unless specifically referenced as a Digital Surface Model (DSM), the generic DEM normally implies elevations of the terrain (bare earth *z*-values) void of vegetation and man-made features (Maune *et al.*, 2001). It is precisely with this meaning that we use the term DEM in this paper.

The diverse possibilities offered by analytical cartography allows us to exploit these DEMs in order to obtain quantitative and qualitative information of great interest, being widely used in hydrological analyses, natural resources management, transport planning, determination of the environmental impact of an activity, calculating the risk of floods in urban zones, military applications, and analysis of the potential erosion of agricultural soil (e.g., Franklin, 2000; Davis and Wang, 2001; Desmet *et al.*, 1999).

At the same time, DEMs are absolutely necessary to generate orthoimages, possibly one of the stellar products offered by modern digital photogrammetry. It is in this field where a very productive integration is taking place between Image Analysis and Geographic Information Systems (GIS). In fact, orthoimages and DEMs are becoming a primary data source for GIS, contributing a fast methodology at a reasonable cost for the actualisation of spatial information which allows the shortening of conventional cartographic actualisation cycles (Baltsavias and Hahn, 1999).

To obtain a good DEM, we need to treat two clearly differentiated phases with great care. On the one hand, the technology employed to acquire sampling points (stereo photogrammetry (Heipke, 1995), conventional topography (Kleim *et al.*, 1999), radargrammetry (Toutin, 2002), laser scanning or lidar (Fricker *et al.*, 2002) which will depend on the real model scale and the sampling density required, among other factors. Second, we must be careful with the selection of an interpolation method to fill in the initial sampling points, as it could considerably affect the quality of the DEM generated. Although one can find very thorough reviews in the literature about the different interpolation methods that exist, e.g., Lam (1983), Robeson (1997), Burrough and McDonnell (1998), there are fewer studies about the efficacy of interpolators applied to the same set of data, the most commendable being those of Franke (1982), Weber and Englund (1992), Weber and Englund (1994), Declerq (1996), and Yang and Hodler (2000).

Department of Agricultural Engineering, Almería University, Ctra. de Sacramento s/n, La Cañada de San Urbano, Escuela Politécnica Superior, 04120 Almería, Spain (faguilar@ual.es, faguera@ual.es, maguilar@ual.es, carvajal@ual.es).

Photogrammetric Engineering & Remote Sensing
Vol. 71, No. 7, July 2005, pp. 805–816.

0099-1112/05/7107–0805/$3.00/0

Thus, in the last three decades Radial Basis Functions (RBF) have emerged as a relevant tool for the approximation theory in mathematical literature, being considered as a highly effective and simple method for the interpolation of multivariant functions starting from the irregular geometry sampling networks (Lazzaro and Montefusco, 2002). The pioneering work developed by Hardy (1971) exhibited a new analytical method of representing irregular surfaces (topographic surfaces) that involved the summation of equations of quadric surfaces having unknown coefficients. Since then, there have been many applications of this approximation method in such diverse fields as photogrammetry, surveying and mapping, geodesy, geophysics, remote sensing, digital terrain modelling, hydrology, signal processing, and artificial intelligence (Mitasova and Mitas, 1993; Rippa, 1999; Li and Chen, 2002).

Conversly, just as some authors indicate (Li, 1992; Gao, 1995; Gao, 1997; Weng, 2002), the morphology of the modelized topographic surface and the sampling density used can have a significant influence on the accuracy of the DEM concerned. In fact, some morphology derived variables, such as average terrain slope, seem to be positively correlated with the increase in global error of the modelized surface (Toutin, 2002; Felicísimo, 1992).

The objectives of this study are: (a) to evaluate, from an exclusively quantitative viewpoint, the effects of terrain morphology, sampling density, and interpolation methods for scattered sample data on the accuracy (RMSE) of interpolated heights in Grid DEM; and (b) to investigate the relationship between the RMSE and such variables as sampling density and terrain ruggedness. The next step in this study would be the development and validation of empirical models which would allow us to estimate the RMSE inherent to the interpolation of a Grid DEM. These models can be used to offer the means to decide how many points should be kept to guarantee the quality requirements of a DEM.

Methodology

In order to achieve the objectives proposed above, a factorial experimental design was carried out. This experimental design allowed us to analyse the influence on the DEM accuracy from factors such as the morphology of the topographic surface, the interpolation method employed, and the number of sampling starting points or sampling density.

Study Sites and Data Sets

The study area is located in Campo de Níjar (Almería), Southeast Spain. The zone represents a semi-arid climate where annual rainfall averages approximately 260 mm.

In order to cover varying terrain morphologies, seven study sites with different topography were chosen from a dry ravine typical of Southeastern Spain to a smooth hillside with an uniform slope. Table 1 summarizes some charasteristics of these different terrain datasets. It includes relief features that are closely connected with terrain variability and roughness, such as standard deviation of slope, mean profile curvature (Mitasova and Hofierka, 1993), and standard deviation of unitary vectors perpendicular to topographic surface. Each study site covered an area of 198 meters by 198 square meters (39,200 m^2).

The DEM for each of the topographic surfaces selected was obtained automatically by means of stereo image matching (Heipke, 1995). Later, a revision and a manually edited version of the DEM were carried out.

The photogrammetric flight presented an approximate scale of 1:5000 and was carried out with a Zeiss RMK TOP15 metric camera using a wide-angle lens with a focal lenght of 153.33 mm. The negatives were digitalized with a Vexcel 5000 photogrammetric scanner with a geometric resolution of 20 μm and a radiometric resolution of 24-bits (8-bits per RGB channel). For the construction of the DEM we employed the module *Automatic Terrain Extraction* of the digital photogrammetric system Leica Geosystems Systems SOCET SET NT® r.4.3.1, obtaining a final DEM in Grid format with a spacing of 2 meters by 2 meters, orthometric elevations, map projection UTM Zone 30, and European Datum 1950.

For better understanding, Figure 1 represents the perspective block diagram of the different topographic surfaces contemplated in this study.

Interpolation Methods Tested

The interpolation methods evaluated are some of those included in the Radial Basis Functions (RBF) group, i.e., Multiquadric, Inverse Multiquadric, Multilog, Natural Cubic Splines, and Thin Plate Splines. Likewise, an interpolator widely used in the modelization of surfaces, Inverse Distance Weighted (IDW), has been introduced in this study for comparison with interpolation methods based on RBF.

Inverse Distance Weighted

Inverse Distance Weighted is one of the most widely used methods for surface modelling. It is based on the intuitive idea that the closest observations must carry more weight in determining the interpolated value in one point. It is an exact and local interpolator which estimates the value of the variable Z in a non-sampling point x_o from the following expression:

$$Z(x_0) = \frac{\sum_{i=1}^{n} w(d_i).z(x_i)}{\sum_{i=1}^{n} w(d_i)} \quad (1)$$

TABLE 1. GENERAL CHARACTERISTS OF THE TOPOGRAPHIC SURFACES STUDIED

Terrain Descriptive Statistics	Flat	Rolling	Flat-Rough	Mountainous	Smooth Hillside	Gorge	Dry Ravine
DEM size (points 2 by 2 m spacing)	10000	10000	10000	10000	10000	10000	10000
Average elevation (m)	166.54	176.94	170.21	215.16	120.25	125.18	47.25
Maximum elevation (m)	170.01	185.57	173.24	237.76	124.71	141.57	65.12
Minimum elevation (m)	163.31	168.32	166.61	192.59	115.65	110.16	36.01
Elevation coeff. of variation (%)	0.97	2.28	0.84	3.98	2.01	5.01	19.57
Average Slope (%)	3.30	9.27	3.30	31.18	4.52	25.45	23.13
Standard deviation of slope (degrees)	0.92	2.42	1.21	6.64	0.46	8.65	11.59
Mean profile curvature	0.021	0.022	0.022	0.031	0.0138	0.035	0.029
Standard deviation of unitary vectors	0.034	0.09	0.039	0.31	0.024	0.285	0.295

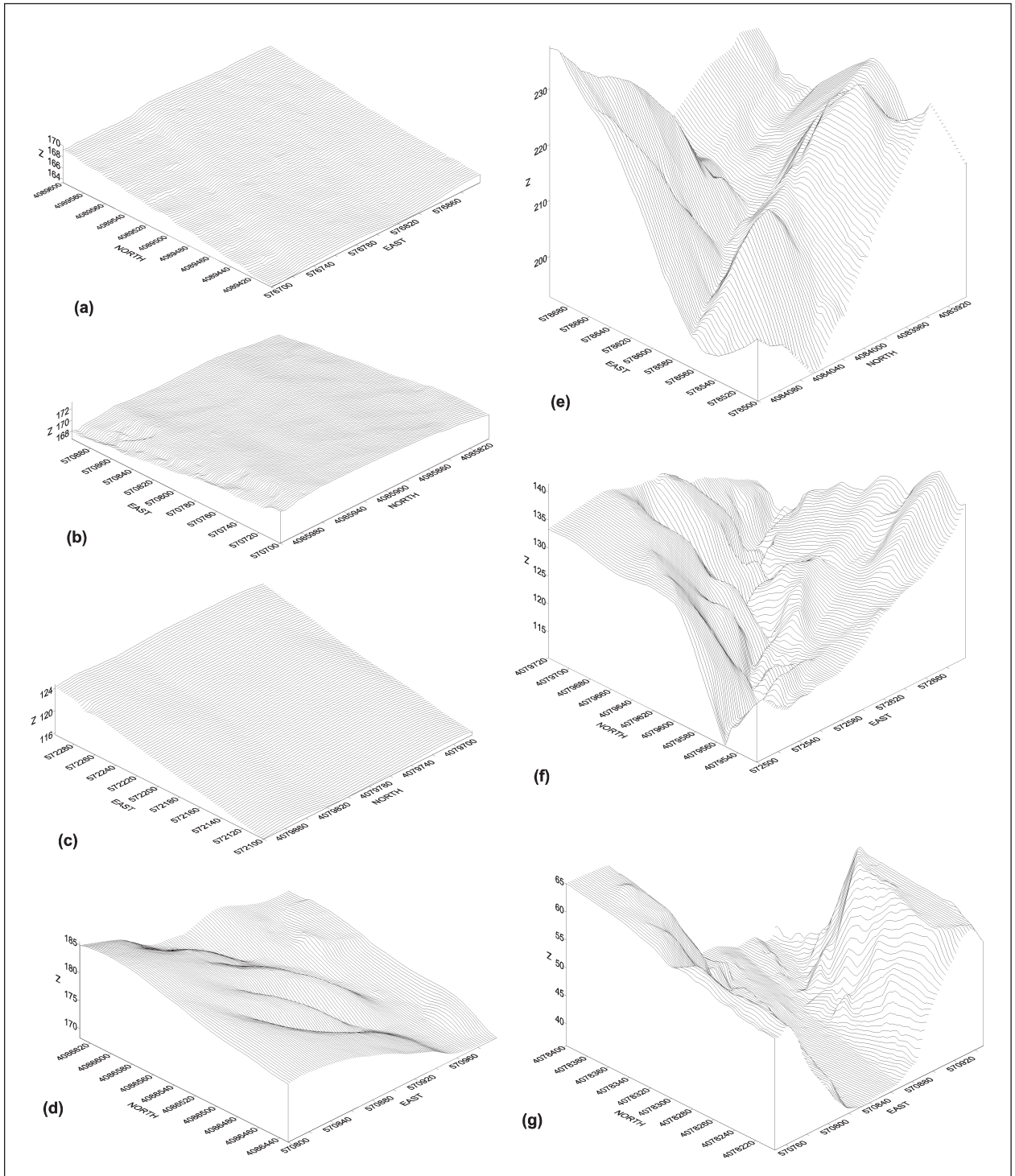

Figure 1. Perspective block diagram of every one of the seven topographic surfaces studied: (a) Flat, (b) Flat rough, (c) Smooth hillside, (d) Rolling, (e) Mountainous, (f) Gorge, and (g) Dry Ravine.

where $w(d_i)$ shows the weight function on the n sampling points which intervene in the calculation, $z(x_i)$ is the elevation of every one of these n points and d_i represents the distance between each point and x_o. With the restriction of $w(d) \to \infty$ if $d \to 0$ the weight functions adopt the general form $w = d^{-u}$. The most common values of the exponent are $u = 1$ and $u = 2$ (Lam, 1983), although some authors establish that exponent 2 usually offers more satisfactory empirical results, besides requiring less computational effort (Declerq, 1996). Obviously, the use of high exponents implies less relative weight for the points which are farthest away from X_o and vice versa.

For this paper we carried out a previous study (Aguilar *et al.*, Unpublished Data, 2002) which determined the

optimum exponent for each sampling density within each analysed morphology, a value which was finally used in later calculations. As a summary of all this, we can indicate that the most frequently repeated optimum exponent was $u = 2$, although in some cases exponents 1 and 3 were preferable. In any case, we must highlight the fact that the results offered through this interpolation method were not very sensitive to the exponent when we moved in a 1 to 3 interval.

Radial Basis Functions

Radial Basis Functions comprise a vast group of exact interpolators which use a basic equation dependent on the distance between the interpolated point and the sampling points. This basic equation must take into account that the interpolation function minimizes an appropiate functional which represents some measure of smoothness of this function. The mathematical background for construction of RBF can be consulted in the work published by Talmi and Gilat (1977). As a rule, the value of variable Z in a point x can be expressed as the sum of two components (Mitasova and Mitas, 1993):

$$Z(x) = \sum_{i=1}^{m} a_i f_i(x) + \sum_{j=1}^{n} b_j . \Psi(d_j) \tag{2}$$

where $\psi(d_j)$ shows the radial basis functions and d_j the distance between each known sample point and x. The "trend" function, $f_i(x)$, can be considered as a member of a basis for the space of polynomials of degree $< m$. The coefficients a_i and b_j need to be calculated by means of the resolution of the following system of $n + m$ linear equations, n being the number of sampling points which intervene in the interpolation of the surface $Z(x)$:

$$Z(x_k) = \sum_{i=1}^{m} a_i f_i(x_k) + \sum_{j=1}^{n} b_j . \Psi(d_{jk}) \quad \text{for } k = 1,2,\ldots,n \tag{3}$$
$$\sum_{j=1}^{n} b_j f_k(x_j) = 0 \qquad \text{for } k = 1,2,\ldots,m.$$

Although the said interpolators were devised for global support, e.g., in the case of the surface spline (Yu, 2001), their application to large volumes of data presents a series of problems, such as the high computational cost, an increase in the numerical instability of the solution found, and the influence of all the sampling points on each interpolated value (Lazzaro and Montefusco, 2002). For overcoming this problem, some authors have suggested an approach based on a segmentation procedure with flexible overlapping neighborhood (Mitasova and Mitas, 1993). We have, therefore, preferred to work with the local support of the eight neighbours closest to the interpolated point, a procedure that, following previous trials carried out by our group (Aguilar *et al.*, 2001; Aguilar *et al.*, Unpublished Data, 2002), usually yields good results in relatively uniform sampling networks, and that coincides with that recommended by other authors (Yang and Hodler, 2000; Robeson, 1997; Weber and Englund, 1994).

Among the various RBFs that can be found in the bibliography, Franke (1982) recommends that the multiquadric as the one providing the best results in terms of the statistical and visual evaluation of the modelized surface. An equation of topography based on multiquadric summation applies a simple geometric concept, where the smoothness and shape of the transition between data points are controlled principally by the characteristics of the basic quadric used in the summation (Hardy, 1971). As an example, when the quadric used is a right circular cone with the vertex located at the x and y coordinates of each sample point, the coefficients b_j associated with each sample point is the asymptotic slope of the cone relative to the x, y plane. The algebraic sign of b_j determines which surface of the cone in two sheets is to be entered into the summation.

In this study we have evaluated, apart from the multiquadric function (MQF), other interesting functions such as multilog (MLF), inverse multiquadric (IMQF), natural cubic splines (NCSF), and thin plate splines (TPSF). The radial basis functions used for each case present the following expressions:

$$\begin{aligned}
&\text{MQF:} && \Psi(d) = \sqrt{d^2 + c^2} \\
&\text{MLF:} && \Psi(d) = \log(d^2 + c^2) \\
&\text{IMQF:} && \Psi(d) = \frac{1}{\sqrt{d^2 + c^2}} \\
&\text{NCSF:} && \Psi(d) = (d^2 + c^2)^{\frac{3}{2}} \\
&\text{TPSF:} && \Psi(d) = (d^2 + c^2) \cdot \log(d^2 + c^2)
\end{aligned} \tag{4}$$

where:
d equals the distance from the point to the node, and c equals the smoothing factor.

The value of parameter c, which depends fundamentally on the number, elevation, and spatial distribution of the sampling points can have a marked influence on the interpolation results obtained (Rippa, 1999). There is no universally accepted method for introducing the smoothing factor, although in the references section there are various empirical type approximations, as those proposed by Hardy (1971) and Franke (1982), together with others of a statistical type where cross-validation techniques are used (Li and Chen, 2002), or recursive algorithms which try to find the value of c which minimizes the global error of the interpolated surface (Rippa, 1999). In our case, we use the latter option, obtaining values close to zero in the cases of MQF and MLF. However, we need very large values working with IMQF, NCSF, and TPSF because a pronounced numerical instability was observed when low smoothing factors were used.

As an example, when c equals 0 in the case of multiquadric function, the associated quadric is a right circular cone, whereas if $c > 0$ the function $\psi(d_j)$ are taken to be the upper sheet of a hyperboloid of revolution.

On the other hand, when we add the first term ("trend" function) of Equation 2 to the MQF, the resulting surface is a multiquadric solution on which the effects of a normally low-degree polynomial are superimposed to reduce the slopes to zero at the desired maximums and minimums (hilltops and depressions). However, when c equals 0 or is small enough (cone or a sharp-nosed hyperboloid) the "trend" function does not improve the accuracy of MQF interpolant (Hardy, 1971). Likewise, Carlson and Foley (1991) observe that adding polynomial precision does not appear to improve the accuracy for MQF and IMQF interpolants. Hence, we decided avoiding the "trend" function in the Equation 2 for every RBF interpolation methods, including MLF, NCSF, and TPSF. This decision involves an important simplification, always desirable, but also implies uncertainty about the accuracy of the final results.

Statistical Evaluation of the Interpolation Grid DEM Accuracy

In Figure 2 we observe the flowchart of the procedure employed for the evaluation of the interpolated Grid DEM accuracy. Because this paper focuses primarily on the assessment of interpolation accuracy in the Grid DEMs interpolated from scattered sample data, the errors inherent in the check points collection are not discussed. In other words, we considered that the check points are free of error (Li, 1992; Gao, 1995).

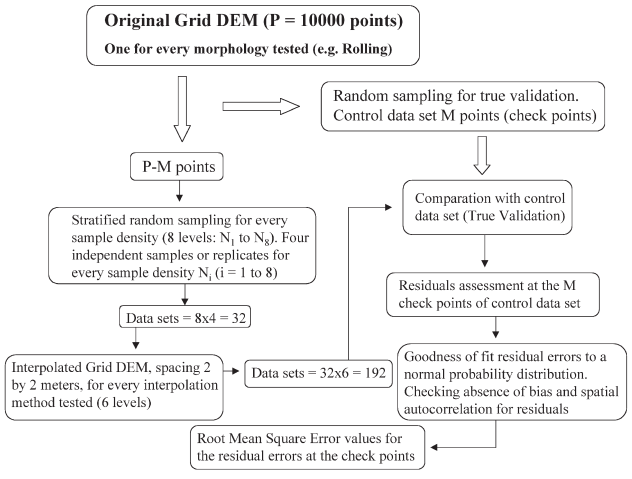

Figure 2. Flowchart of the scheme used to evaluate interpolated Grid DEM accuracy.

It seems obvious that the inclusion of more check points in the data set will lead to a more reliable results. However, in many practical applications, a large number of check points may be costly to produce. Therefore, an initial number of 400 randomly selected point were extracted from the original Grid DEM corresponding to each study site or morphology (Table 1). These points were used as check points for the adjustment degree of the interpolated Grid DEM by comparison with the real model, a technique known as *true validation* (Voltz and Webster, 1990).

The most widely used global accuracy measure for evaluating the performance of DEMs is the Root Mean Square Error (RMSE) (Li, 1988; Yang and Hodler, 2000):

$$\text{RMSE} = \sqrt{\frac{\sum_{i=1}^{n} (Z_i^{estimated} - Z_i^{real})^2}{n}} \quad (5)$$

where $Z^{\text{estimated}}$ minus Z^{real} is the residual at each check point, and n the number of points. Thus, the RMSE was calculated over 400 check points extracted from each morphology. It is worth pointing out that with a 400 point sampling size, we can expect errors in the DEM global error measure of approximately 3.54 percent (Li, 1991), values which are sufficient to achieve the objectives of this study.

Some authors have proposed to consider other measures of error apart from the RMSE, for example the 95-percentile method. It is far simpler than the RMSE process for computing vertical accuracy, and it does not assume that all 100 percent of the residuals must have a normal distribution. In fact, it works well when 95 percent or more of the check points present a normal distribution (Daniel and Tennant, 2001). But, if we can prove that our population of errors is normal (i.e., no gross errors or outliers), the conclusions will be similar irrespective of the measure of the error used.

Once the check points had been extracted, a stratified random sampling was carried out, with four repetitions per sampling density and morphology in order to guarantee the homogeneous distribution of sampling points within the scope of the original Grid DEM (Burrough and McDonnell, 1998). The sampling densities obtained were those showed in Table 2, i.e., from $N1 = 96$ points to $N8 = 4{,}800$ points.

The modeled surface was generated from each sampling density and by each interpolation method using the software SURFER® 8.01 (Golden Software, 2002), which allows the storage of interpolated data in a Grid type format, the size of which can be defined by the user. In our case, we used 100 nodes by 100 nodes grids. As the six interpolation methods work on local support, it was necessary to indicate the number of closest neighbors that would intervene in the calculation of the interpolated value in each node and their search method (simple, quadrant, and octant searching). Following previous trials carried out by our group (Aguilar *et al.*, 2001; Aguilar *et al.*, unpublished data, 2002), the simple search of the eight closest neighbours was used.

After obtaining the residuals in each case and before finding the RMSE, we checked that their distribution was approximate to a normal distribution with a zero mean. That is to say, that all systematic errors and outliers have been removed and the estimation was unbiased. For this purpose, the Smirnov-Kolmogorov test (Royston, 1982) was used and the interval of the residuals average was determined with a confidence level of 95 percent.

It is also important to know whether interpolation error may be spatially autocorrelated. In fact, this property of DEM error has been reported by several authors (Wood, 1996; Weng, 2002). If error at the check points are in fact not independent, we could state that the true sample size is less than 400. Therefore, the use of a data set of 400 spatially autocorrelated residuals would lead to a RMSE variability lower than it should be, and that the F-statistics in the ANOVA tests would be inflated. Thus, we checked the degree of spatial autocorrelation for every residuals data set with a semivariogram, finding a clearly defined spatial structure like we can see in Figure 3a. It shows the experimental standardized semivariogram and the fitted spherical model corresponding to the following variables: Sample density = $N1$ (96 points), Flat terrain, MLF interpolant and 400 check points. The curve that has been fitted through the experimentally-derived data points displays a typical transitional semivariogram with range, nugget, and sill. The range, approximately 20 meters in this case, gives us an answer to the question posed. If the distance separating two check points is greater than the range, then residuals measured at those check points are not spatially autocorrelated. In fact, in Figure 3b we can see the experimental standardized semivariogram corresponding to the same case showed in Figure 3a, but now only using 60 check points separated by a distance vector greater than 20 meters. We can observe the absence of spatial

TABLE 2. SAMPLE DENSITIES TESTED, INDICATED BY $N1$ TO $N8$ ARE COMPOSED OF SCATTERED SAMPLE DATA FROM STRATIFIED RANDOM SAMPLING (ES = EQUIVALENT SPACING)

	Sample Density N							
	N_1	N_2	N_3	N_4	N_5	N_6	N_7	N_8
Points	96	192	480	960	1440	1920	2880	4800
ES (m)	20.2 × 20.2	14.3 × 14.3	9.0 × 9.0	6.5 × 6.5	5.2 × 5.2	4.5 × 4.5	3.7 × 3.7	2.8 × 2.8

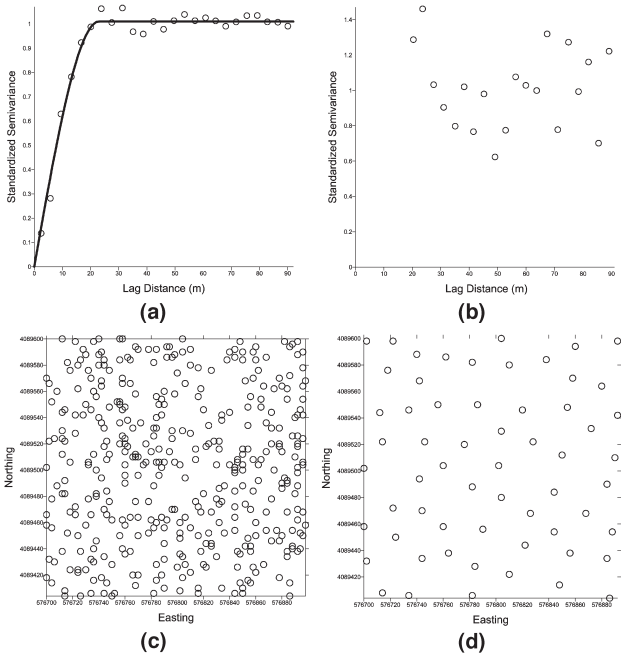

Figure 3. (a) Experimental standardized semivariogram (circles) and the fitted spherical model (solid line) for sample density $N = 96$ points, flat terrain, MLF interpolant and 400 check points, (b) Experimental standardized semivariogram (circles) for sample density $N = 96$ points, flat terrain, MLF interpolant and 60 check points separated by a distance greater than 20 meters, (c) *x-y* scatter plot of 400 check points sampling net, and (d) *x-y* scatter plot of 60 check points sampling net.

structure or autocorrelation. Therefore, residuals measured at these check points are not spatially autocorrelated. The *x-y* scatter plots of check points sampling net is showed in Figure 3c (400 check points) and Figure 3d (60 check points). Finally, the information in the different semivariograms corresponding to all experimental data sets has been used to help optimize check points sampling. So, an average scheme based on 60 points separated by a distance greater than 20 meters was used. Since the number of check points have been changed from 400 to 60, the expected error in the DEM global error measure was calculated again, finding a value of around 9.20 percent (Li, 1991) which is still sufficient to achieve the objectives of this study.

The RMSE was the variable observed or dependent on the general variance analysis of the factorial model designed. The variation sources analysed were morphology, interpolation method and sampling density, as well as every interaction among them. When the analysis results of the variance were significant, we proceeded to the separation of averages using the Duncan multiple rank test.

The whole procedure described above was programmed with the SCRIPTER® module, included in SURFER® 8.01 (Golden Software, 2002), which allows the use of the tool Active X Automation to work with the SURFER® modelization engine in an environment that is compatible with Visual Basic®.

Results and Discussion

Qualitative Analysis

First, we note that some RBF interpolants tested, such as IMQF, NCSF, and TPSF present unexpectedly large discrepancies between some of the check points elevations and the elevations interpolated from our sampling points dataset. Although the objective of this article is to evaluate the accuracy of interpolated heights in Grid DEMs from an exclusively quantitative viewpoint, the use of qualitative studies based on visualization methods can be considered as an effective tool for analyzing elevation model accuracy, because its flexibility in interpretation and because easily convey the significance of data uncertainty to the DEM users (Wood and Fisher, 1993).

This previous qualitative study of the efficiency of the six interpolators examined yielded some especially encouraging results for the continuation of our work. In fact, like the quantitative analysis indicated, those interpolants based on RBF such as IMQF, NCSF, and TPSF presented a pronounced numerical instability for most of the morphologies and sampling densities used. In Table 3 we can see the cases of flat and mountainous terrain, where the elevation rank of

TABLE 3. COMPARATION BETWEEN ELEVATION RANK OF THE SAMPLE POINTS AND INTERPOLATED GRID DEM USING SOME RBF METHODS

		Elevation Rank of the Interpolated Points (m)							
		Elevation Rank of the Sample Points (m)		IMQF		NCSF		TPSF	
Terrain	Sample Density	Z min.	Z max.	Z min.	Z max.	Z min.	Z max.	Z min.	Z max.
Flat	N_1	163.46	169.63	−2546.29	1162.98	163.42	169.96	163.33	169.90
	N_2	163.61	169.89	−619.80	708.39	163.14	170.05	68.49	172.40
	N_3	163.34	169.87	−2092.84	977.58	126.29	185.66	161.72	183.98
	N_4	163.44	170.00	−553.53	249888	90.99	182.19	123.23	176.18
	N_5	163.37	169.97	−362.44	1992.68	144.20	252.21	−1586.3	519.12
	N_6	163.31	169.94	−1621.22	109758	135.78	200.73	−56.63	482.16
	N_7	163.36	170.01	−475.82	1883.58	132.95	200.20	144.49	284.64
	N_8	163.31	169.99	−2492.72	527.84	152.29	182.48	111.89	192.39
Mountainous	N_1	196.04	231.17	−10580.70	2504.48	193.56	232.68	194.37	236.84
	N_2	195.37	237.28	−29258.20	8260.40	194.60	237.28	194.63	298.86
	N_3	192.65	237.50	−38838.70	12695.40	57.71	492.16	−561.59	363.60
	N_4	192.65	237.40	−2436.43	4885.97	−30.77	308.26	139.91	325.12
	N_5	193.06	237.40	−6909.89	10360.54	−19.20	322.88	118.65	543.36
	N_6	192.65	237.50	−22830.40	17660.58	−115.77	17200.2	−384.45	1596.52
	N_7	192.59	237.40	−1172.94	5926.75	94.68	312.52	−33.32	3230.13
	N_8	192.65	237.52	190.32	236.78	160.00	267.33	88.83	298.42

the interpolated points surpasses, sometimes remarkably, e.g., IMQF, the elevation rank of the sampling points.

In Figure 4, we present the perspective block diagrams for true DEM (i.e., using all of the 10,000 sample points available) and interpolated Grid DEM for the RBF methods. In each case the *N*5 (1,440 points) sampling density extracted from mountainous terrain was used as a basis. As can be seen, whilst the MQF (Figure 4b) and MLF (Figure 4c) methods offer smoothed perspective block diagrams very similar to that obtained with the true DEM (Figure 4a), NCSF and TPSF present a more irregular 3D projection with numerous "blunders." IMQF is the poorest interpolator in the previous qualitative comparison, although it is not shown in Figure 4 because the "blunders" are too large to be displayed with the vertical scale used. In any case, and for these last three interpolators, the interpolated values were highly influenced by the geometry of the sampling points network.

But, what is the reason for these outliers? Splines, such as natural cubic splines or thin plate splines, are a general class of interpolation techniques that use a mathematical formula to create a surface that minimizes the overall surface curvature resulting in a smooth surface that passes through the sample points. This method is very useful for creating elevation models of areas with gently varying terrain and smooth slope transitions. However, it is very sensitive and not suitable for sharp changes in value over short distances, such as steep cliffs or man-made features. In such situations, it has a tendency to over-exaggerate the value of neighboring sample points (Mitasova and Mitas, 1993). In the case of TPSF, overshoots appear due to the plate's stiffness. The stiffness of the plate can be suppressed by including first derivatives to the smooth seminorm, which enables the character of the interpolation surface be tuned from thin plate to membrane (Mitas and Mitasova, 1988). Likewise, we must remember that we decided avoiding the "trend" function in the Equation 2 for every RBF interpolation methods. From Equations 2 and 3, we can see that a surface developed by adding polynomial terms to the radial basis surface can achieve polynomial precision, i.e., a first polynomial trend is extracted from the data and the radial basis function is applied to the residuals only. In other words, removing the "trend" function with some RBF methods often imposes a strong artifact in the resulting generated surface to avoid the extreme change in curvature which really does exist.

In the case of NCSF and TPSF, the elevation rank of the interpolated points is similar to the elevation rank of the sample points when sample density is low, mainly in flat terrain. But, when sample density is greater, extremes differences between closely neighboring data values can appear, mainly in mountainous terrain. Then the system of interpolation equations could be numerically unstable or even unsolvable. When this condition occurs and the data set contains such extreme data pairs, we must consider increasing the tolerance for filtering duplicate points, adding the "trend" function or increasing the smoothing factor. We decided to increase the smoothing factor. Effects of adding the "trend" function will be studied in future work.

As observed by Carlson and Foley (1991) or Rippa (1999), the value of the optimal smoothing factor strongly depends on the approximated function used. We note that IMQF, NCSF, and TPSF data presented in Table 3 and Figure 4 corresponding to a squared smoothing factor values (c^2) around 4 m^2. We show, numerically, that the value of optimal c^2 (the value that minimizes the interpolation error) presents different behaviour depending on the RBF evaluated (Figure 5). RBF Multilog (and also RBF Multiquadric) presents an optimal smoothing factor close to zero with a lower RMSE when c^2 decrease. However, IMQF, NCSF, and TPSF only show a regular relationship between RMSE and c^2 when the artifacts or "blunders" are removed, but it does not occur until c^2 is greater than 2,300 m^2 to 2,500 m^2, in the case of IMQF or NCSF, and 700 m^2, for TPSF interpolant. In other words, we need very large c^2 values working with IMQF, NCSF, and TPSF because a pronounced numerical instability is observed when used low smoothing factors. It should be observed that a highly smoothed factor will produce a very smoothed modelized surface which will probably be very far removed from the geometry of the real surface. In fact, we have found that IMQF, NCSF, and TPSF, without the "trend" function but using large smoothing factors for avoiding instability, performed worse than MQF or MLF interpolants working in the same conditions, particularly when the terrain becomes steeper.

In view of these results, we decided to continue with the quantitative analysis of the data, cutting down to three the levels of the interpolation method variable: Multiquadric, Multilog, and Inverse Distance Weighted.

Quantitative Analysis

The general variance analysis of the factors examined allows us to check the significant influence ($p < 0.01$) of the variables terrain morphology: (A) sampling density, (B) interpolator, and (C) in the RMSE of a grid DEM (Table 4). A great part of the global variance of the model is explained by the factors morphology and sampling density, closely followed by the interpolation method. It should be noted that, although all interactions are significant excepting $A \times B \times C$, the interaction between morphology and sampling density appears to be the most consistent, confirming the suitability of implanting the method called Progressive Sampling in the automatic generation of DEM (Makarovic, 1973), a technique which increases the number of sampling points in rugged topography zones. Although this technique can produce highly redundant sampled data in the proximity of abrupt changes in terrain surface, it can be avoided by sampling these abrupt changes selectively. This optimal procedure is called Composite Sampling (Makarovic, 1979).

Within the morphology factor, we can find four groups of topographic surfaces where statistical differences are significant ($p < 0.05$). The less-rugged terrain presents an average RMSE (including all sample densities and interpolation methods) which is very close to or below 7.6 cm, while as the terrain becomes more undulating, we observe a significant increase in the RMSE, reaching its highest value at 61.6 cm in the case of the morphology known as "Gorge" (Figure 6). In this way, Gao (1995) observed that gentle terrain was more accurately represented than complex terrain by DEMs of the same resolution.

Correlation coefficient between average RMSE for each morphology and the different empirical measures showed in Table 1 lead to propose standard deviation of unitary vectors perpendicular to topographic surface, such as the best estimation of terrain roughness ($r = 0.99$) for our dataset. Of course, we need to develop more detailed studies to confirm this finding.

Means separation for the variation source interpolation method (Table 5) has yielded significant results ($p < 0.05$) which highlight the weakness of the IDW method with regard to the RBF methods. The greatest problem presented by IDW is likely to be that the interpolated heights are weighted averages that always take values between the maximum and minimum basis points (Lam, 1983) which reduces its efficacy to estimate the highest or lowest levels of a topographic surface when these levels do not belong to the set of sampling points.

The influence pattern of the RBF interpolation methods on the accuracy of the DEM generated has been slightly

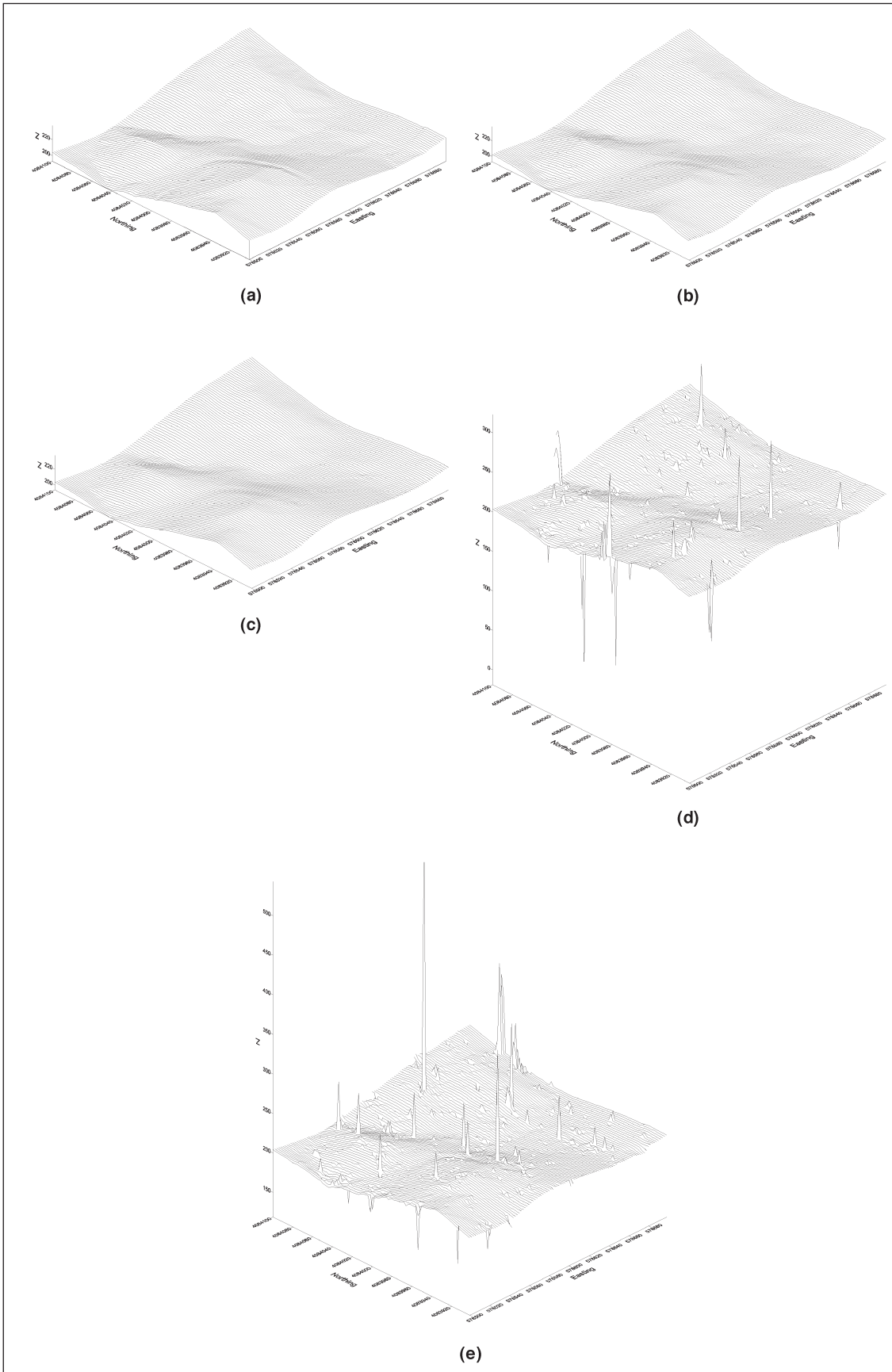

Figure 4. Perspective block diagram for true DEM and interpolated Grid DEMs: (a) True model with 10,000 sample points, (b) MQF ($c^2 = 0$ m^2), (c) MLF ($c^2 = 0.1$ m^2), (d) NCSF ($c^2 = 4$ m^2), and (e) TPSF ($c^2 = 4$ m^2). Note: All cases for a mountainous terrain and sample density $N = 1440$ points.

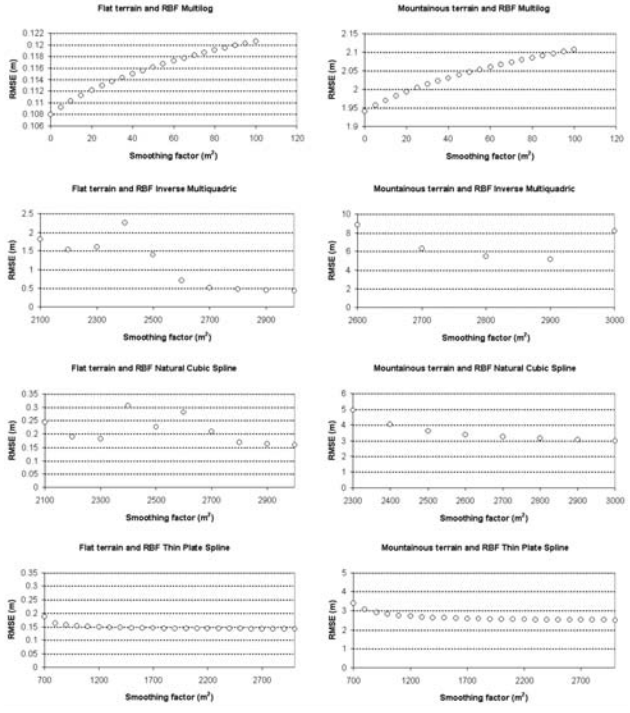

Figure 5. Relation between squared smoothing factor (c^2) and RMSE for flat and mountainous terrain using some RBF interpolation methods.

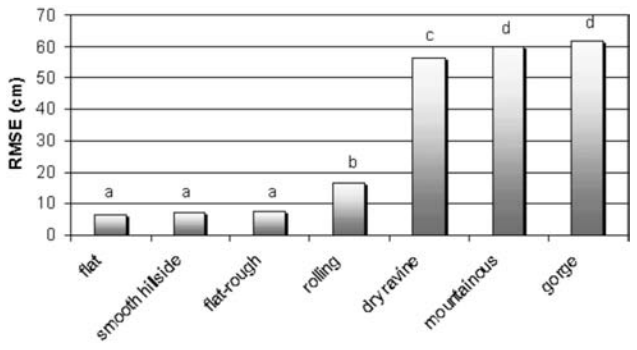

Figure 6. Means separation for morphology. Vertical bars with different letters indicate significant differences ($p < 0.05$) between morphologies.

TABLE 4. GENERAL ANALYSIS OF VARIENCE FOR THE RMSE OBSERVED DATA (DEPENDENT VARIABLE)

Source	Degrees of Freedom	Sums of Squares	Mean Square	F-test	P-value
(A) Morphology	6	41.46	6.91	1382.49	P <0.01
(B) Sample density	7	35.73	5.10	1021.42	P <0.01
(C) Interpolation method	2	2.68	1.34	267.91	P <0.01
Interaction A × B	42	24.65	0.58	117.44	P <0.01
Interaction A × C	12	1.61	0.13	26.97	P <0.01
Interaction B × C	14	0.47	0.03	6.79	P <0.01
Interaction A × B × C	84	0.49	0.006	1.18	0.1498
Residual	504	2.52	0.005		

TABLE 5. RMSE VALUES ACCORDING TO THE VARIABLES INTERPOLATION METHOD AND MORPHOLOGY. FOR A GIVEN ROW, DIFFERENT LETTERS BETWEEN DATA IN DIFFERENT COLUMNS INDICATE SIGNIFICANT DIFFERENCES ($P < 0.05$)

	IDW	MLF	MQF
	RMSE (cm)		
General Means Separation Test	39.72a	27.68b	25.30c
Morphology			
Flat	8.80a	5.82b	5.64b
Smooth hillside	12.20a	3.92c	5.76b
Flat-rough	9.27a	6.90b	6.58b
Rolling	22.25a	14.71b	13.34c
Dry ravine	72.63a	52.11b	44.27c
Mountainous	80.04a	51.01b	48.87b
Gorge	72.87a	59.30b	52.65c

different with regard to the basis morphology. For smooth terrain, MLF presents a similar performance to that of MQF, and even higher in the case of smooth hillside terrain. However, as the terrain becomes steeper MQF works significantly better than MLF (Table 5). Franke (1982) compared the majority of the interpolation methods for scattered data sets available at that time, and Hardy's Mutiquadrics were ranked as the best. The studies carried out by Yang and Hodler (2000) lead to the same conclusion. It is more difficult to find references about the efficacy of the Multilog Function interpolation method, which in any case, and judging from the results obtained in this study, seems to be more accurate than the classic Inverse Distance Weighted.

In Figure 7 we can explore how the inherent error patterns of the stereo photogrammetry influence the performance of the interpolation methods tested. As MQF seems to be significantly more accurate than MLF and IDW when sample density decrease and the terrain becomes steeper (dry ravine and gorge in Figure 7), it would be proposed like the more effective interpolation method for filling the sampling gaps produced where stereo photogrammetry methods can not provide reliable measurements (such areas as shadows, occlusions, and poor-texture).

Finally, as observed by Makarovic (1979), Li (1992) and Gao (1995; 1997), sample density also had a significant influence on the accuracy of the Grid DEMs generated. Means separation for the variable sample density can be observed in Figure 8, showing a significant ($p < 0.05$) decrease in the RMSE as the sample density increases in most levels studied. Similar behavior is described by Gao (1997) when observed that the accuracy of the DEMs decreases moderately at an intermediate sample density, but sharply at low sample density for all three terrain types tested.

In fact, it is found that the relationship between the RMSE and the sampling density N is adjusted to a decreasing potential function (Equation 6), being N the number of sampling points used for creating the DEM and SDZ the standard deviation of the heights of the M check points used for accuracy estimation. In any case, the

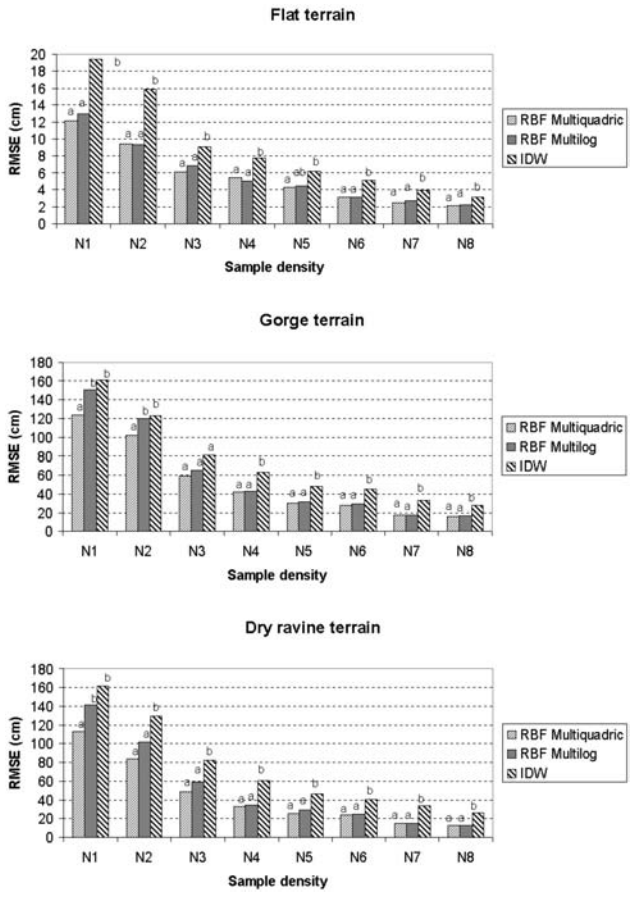

Figure 7. RMSE values according to the variables sample density (*N*1 to *N*8) and interpolation method (MQF, MLF, and IDW) for three of the different morphologies studied. For a given sample density, vertical bars with different letters indicate significant differences ($p < 0.05$) between interpolation methods.

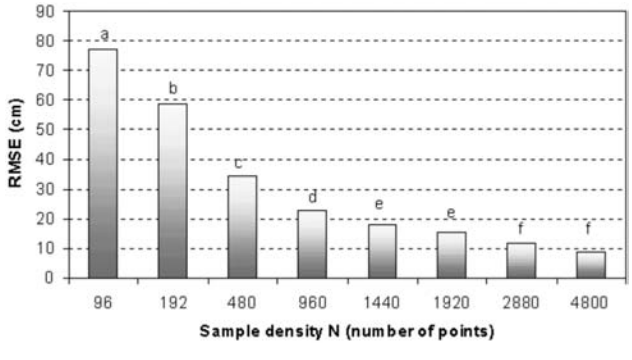

Figure 8. Means separation for sample density. Vertical bars with different letters indicate significant differences ($p < 0.05$) between sample densities.

interpolated Grid DEM was generated using Multiquadric RBF interpolator.

$$\frac{\text{RMSE}}{\text{Sdz}} = 0.1906\left(\frac{N}{M}\right)^{-0.5684}. \quad (6)$$

The adjustment soundness of this model is quite remarkable, with a regression coefficient of $R^2 = 0.8578$. Notice that the regression weights differently the points coming from different terrain morphology because of the factor SDZ, which is large for mountains and smaller for flat terrains.

For practical purposes, and starting from the model devised, we can infer for our rolling terrain (SDZ = 415 cm) that decreasing the number of sampling points by 98 percent ($N = 200$ points) with regard to the original 10,000 points, the increase in the RMSE is in the order of 35.6 cm. However, if the decrease is of 80 percent ($N = 2000$ points), the RMSE will only increase to an average value of 6.5 cm. This result is crucial, since at the moment the problem does not lie in obtaining the data of a DEM, a phase that has reached a remarkable degree of development, (e.g., Fricker *et al.*, 2002; Paparoditis and Dissard, 2002), but in handling and maintaining up to date such an amount of information (Graham *et al.*, 2001) using structures which will allow its efficient integration and exploitation in GIS or CAD applications. In the majority of cases it is preferable to have an optimised DEM adapted to our needs, that is to say, without excess information, than to have a vast amount of data the handling of which will just create difficulties for us. Furthermore, such an enormous amount of data inevitably involves some redundancy.

However, if any DEM producer has a DEM already described in a regular grid or raster format, and faces the problem of use less disk to store it, they could also use data compressión techniques such as JPEG (Fourier transform) or JPEG2000 (Wavelets). So, we think that the most interesting application of Equation 6 is the one of a DEM producer who will create a DEM using scattered data. They should decide the amount of RMSE they are willing to accept and how many sampling points (measured on the ground) are necessary.

Of course, the formula proposed in Equation 6 is purely empirical, and it must be validated against other datasets. Therefore, the next step in this study would be the development and validation of a series of empirical bivariant models which would allow us to estimate the RMSE inherent to the interpolation of a Grid DEM in terms of such variables as sampling density and terrain morphology. Thus, proposals about empirical measures of terrain variability and roughness would be welcome. Some authors have proposed many parameters of terrain roughness such as mean slope (Balce, 1987), the harmonic vector magnitude (Ayeni, 1982), fractal dimension (Goodchild and Mark, 1987), Laplacian operator (Makarovic, 1979), or variance of unitary vectors perpendicular to topographic surface (Felicísimo, 1992). These parameters would allow the characterisation of the degree of roughness in a topographic surface in order to include this information in a predictive model of the accuracy of interpolated heights in Grid DEM. These empirical models would allow us to find out *a priori* the cost, expressed as an increase in RMSE, of a reduction in the number of sampling points for the generation and storage of a DEM.

Conclusions

The results obtained in this study allow us to conclude that terrain morphology, sampling density of the points observed and the interpolation method have a significant bearing on the accuracy of interpolated heights from scattered data in Grid Digital Elevation Models. The global error of the aforesaid models was estimated through the root mean square error taken from an appropriate check points sample. For example, it is important

to check the absence of spatially autocorrelated errors for avoiding that the F-statistics in the ANOVA tests will be inflated.

The factor with the greatest incidence on the quality of the interpolation was morphology, followed by sampling density and interpolation method. The interaction between morphology and sampling density appeared to be the most consistent, confirming the suitability of implanting Progressive Sampling method in the automatic generation of DEMs.

Interpolation by Multiquadric radial basis functions with local support proved to be more accurate than the one based on logarithmic functions in the case of undulating and mountainous terrain, yielding similar results in flat or low roughness terrain. Multiquadric radial basis function provided significantly better interpolation than Multilog function working with low sample densities and steeper terrain. So it would be proposed similar to the more reliable interpolation method for filling the sampling gaps produced, where stereo photogrammetry methods can not provide reliable measurements.

The classic method Inverse Distance Weighted clearly proved to be less appropriate than the two previous ones in any case.

Conversly, the three interpolation methods based on the radial basis functions studied, i.e., Inverse Multiquadric, Natural Cubic Splines, and Thin Plate Splines showed a high level of numerical instability when used low smoothing factors. This fact was highlighted in the case of the Inverse Multiquadric Function with the generation of numerous artifacts or "blunders." We also have found that Inverse Multiquadric, Natural Cubic Splines, and Thin Plate Splines, without the "trend" function but using large smoothing factors for avoiding instability, performed worse than Multiquadric or Multilog interpolants working in the same conditions, particularly when the terrain became steeper. Perhaps it could be explained because a highly smoothed factor will produce a very smoothed modelized surface which will probably be far removed from the geometry of the real surface. In future work, we will study the effects of adding the "trend" function to these three interpolation methods.

The results obtained in this study allow us to observe the possibility of establishing empirical relationships between the RMSE expected in the interpolation of a Grid DEM and such variables as sampling density, terrain ruggedness, and the interpolation method used among others that could be added. For example, we have showed that the relationship between the RMSE and the sampling density is adjusted with remarkable approximation to a decreasing potential function. Therefore, it would be possible to establish *a priori* the optimum grid size required to generate a DEM of a particular accuracy with the economy in computing time and file size that this would satisfy the digital flow of the mapping information. At the same time, they would also be very useful for establishing adaptative sampling strategies with regard to the morphology of the topographic surface that is being modeled.

Acknowledgments

The authors are grateful to the Consejería de Agricultura y Pesca of the Andalusia Government for financing this work through Project: "Cartografía básica para la redacción del proyecto de red de riego del Campo de Níjar (Almería)". Thanks are also due to Professor J. Delgado and Professor J. Cardenal from the University of Jaén (Spain). The kind comments and suggestions made by three anonymous reviewers are also very appreciated.

References

Aguilar, M.A., F.J. Aguilar, F. Agüera, and F. Carvajal, 2001. Evaluación de diferentes técnicas de interpolación espacial para la generación de modelos digitales de elevación del terreno agrícola, *Mapping*, 2001(74):72–88.

Ayeni, O.O., 1982. Optimum sampling for digital terrain models: A trend towards automation, *Photogrammetric Engineering & Remote Sensing*, 48(11):1687–1694.

Balce, A.E., 1987. Determination of optimum sampling interval in grid digital elevation models (DEM) data acquisition, *Photogrammetric Engineering & Remote Sensing*, 53(3):323–330.

Baltsavias, E.P., and M. Hahn, 1999. Integration of image analysis and GIS, *International Archives of Photogrammetry and Remote Sensing*, 32(part 7-4-3W6):12–19.

Burrough, P.A., and R.A. McDonnell, 1998. *Principles of Geographical Information Systems*, Oxford University Press, New York, 333 p.

Carlson, R.E., and T.A. Foley, 1991. The parameter R^2 in multiquadric interpolation, *Computers Mathematics Applications*, 21(9):29–42.

Daniel, C., and K. Tennant, 2001. DEM quality assessment, *Digital Elevation Model Technologies and Applications: the DEM Users Manual* (D.F. Maune, editor), American Society for Photogrammetry and Remote Sensing, Bethesda, Maryland, pp. 395–440.

Davis, C.H., and X. Wang, 2001. High-Resolution DEMS for urban applications from NAPP photography, *Photogrammetric Engineering & Remote Sensing*, 67(5):585–592.

Declercq, F.A.N., 1996. Interpolation methods for scattered sample data: accuracy, spatial patterns, processing time, *Cartography and Geographic Information Systems*, 23(3):128–144.

Desmet, P.J.J., J. Poesen, G. Govers, and K. Vandeale, 1999. Importance of slope gradient and contributing area for optimal prediction of the initiation and trajectory of ephemeral gullies, *Catena*, 37(3–4):377–392.

Felicísimo, A.M., 1992. *Digital Terrain Models and Their Application to Environmental Sciences*, Ph.D. Thesis, University of Oviedo, Spain, 235 p.

Franke, R., 1982. Scattered data interpolation: tests of some methods, *Mathematics of Computation*, 38(157):181–200.

Franklin, W.R., 2000. Applications of analytical cartography, *Cartography and Geographic Information Science*, 27(3): 225–237.

Fricker, P., F. Gervaix, F. Llorens, J. Delgado, and J. Cardenal, 2002. Utilización de sensores aerotransportados para la generación de MDT y ortofotografías: LH ADS40 y LH ALS40, *Proceedings of the Fourteenth International Symposium on Graphic Engineering*, 05–07 June, Santander, Spain, pp. 527–536.

Gao, J., 1995. Comparison of sampling schemes in constructing DTMs from topographic maps, *ITC Journal*, 1:18–22.

Gao, J., 1997. Resolution and accuracy of terrain representation by grid DEMs at a micro-scale, *International Journal of Geographical Information Science*, 11(2):199–212.

Golden Software, Inc., 2002. Surfer 8 Users' Guide, Golden Software Inc., Golden, Colorado, 640 p.

Goodchild, M.F., and D.M. Mark, 1987. The fractal nature of geographic phenomena, *Annals of the Association of American Geographers*, 77(2):265–278.

Graham, L., N. Dahman, and B. Herman, 2001. Enterprise digital terrain modeling, Z/I Imaging White Papers, URL: http://www.ziimaging.com/library.htm, (last date accessed: 31 March 2005).

Hardy, R.L., 1971. Multiquadric equations of topography and other irregular surfaces, *Journal of Geophysical Research*, 76(8):1905–1915.

Heipke, C., 1995. State-of-the-art of digital photogrammetric workstations for topographic applications, *Photogrammetric Engineering & Remote Sensing*, 61(1):49–56.

Kleim, R.F., A.E. Skaugset, and D.S. Bateman, 1999. Digital terrain modeling of small stream channels with a total-station theodolite, *Advances in Water Resources*, 23(1):41–48.

Lam, N.S., 1983. Spatial interpolation methods: A review, *The American Cartographer*, 10(2):129–149.

Lazzaro, D., and L.B. Montefusco, 2002. Radial basis functions for the multivariate interpolation of large scattered data sets, *Journal of Computational and Applied Mathematics*, 140(1–2):521–536.

Li, J., and C.S. Chen, 2002. A simple efficient algorithm for interpolation between different grids in both 2D and 3D, *Mathematics and Computers in Simulation*, 58(2):125–132.

Li, Z., 1988. On the measure of digital terrain model accuracy, *The Photogrammetric Record*, 12(72):873–877.

Li, Z., 1991. Effects of check points on the reliability of DTM accuracy estimates obtained from experimental tests, *Photogrammetric Engineering & Remote Sensing*, 57(10):1333–1340.

Li, Z., 1992. Variation of the accuracy of digital terrain models with sampling interval, *The Photogrammetric Record*, 14(79):113–128.

Makarovic, B., 1973. Progressive sampling for digital terrain models, *ITC Journal*, 1973(3):397–416.

Makarovic, B., 1979. From progressive to composite sampling for digital terrain models, *Geo-Processing*, 1:145–166.

Maune, D.F., S.M. Kopp, C.A. Crawford, and C.E. Zervas, 2001. Introduction, *Digital Elevation Model Technologies and Applications: the DEM Users Manual* (D.F. Maune, editor), American Society for Photogrammetry and Remote Sensing, Bethesda, Maryland, pp. 1–34.

Mitas, L., and H. Mitasova, 1988. General variational approach to the interpolation problem, *Computers and Mathematics with Applications*, 16:983–992.

Mitasova, H., and L. Mitas, 1993. Interpolation by regularized spline with tension: I, Theory and implementation, *Mathematical Geology*, 25(6):641–655.

Mitasova, H., and J. Hofierka, 1993. Interpolation by regularized spline with tension: II, Application to terrain modeling and surface geometry analysis, *Mathematical Geology*, 25(6):657–669.

Paparoditis, N., and O. Dissard, 2002. Generation of digital terrain and surface models, Data acquisition from visible images, *Digital Photogrammetry* (M. Kasser and Y. Egels, editors), Taylor & Francis, Inc., New York, New York, pp. 168–220.

Rippa, S., 1999. An algorithm for selecting a good value for the parameter c in radial basis function interpolation, *Advances in Computational Mathematics*, 11(2–3):193–210.

Robeson, S.M., 1997. Spherical methods for spatial interpolation: Review and evaluation, *Cartography and Geographic Information Systems*, 24(1):3–20.

Royston, J.P., 1982. Expected normal order statistics (exact and aproximate), *Applied Statistics*, 31:161–165.

Talmi, A., and G. Gilat, 1977. Method for smooth approximation of data, *Journal of Computational Physics*, 23:93–123.

Toutin, T., 2002. Impact of terrain slope and aspect on radargrammetric DEM accuracy, *ISPRS Journal of Photogrammetry and Remote Sensing*, 57(3):228–249.

Voltz, M., and R.A. Webster, 1990. A comparison of kriging cubic splines and classification for predicting soil properties from sample information, *Journal of Soil Science*, 41(3):473–490.

Weber, D., and E. Englund, 1992. Evaluation and comparison of spatial interpolators, *Mathematical Geology*, 24(4):381–391.

Weber, D., and E. Englund, 1994. Evaluation and comparison of spatial interpolators II, *Mathematical Geology*, 26(5):589–603.

Weng, Q., 2002. Quantifying uncertainty of digital elevation models derived from topographic maps, *Advances in Spatial Data Handling* (D. Richardson and P. van Oosterom, editors), Springer-Verlag, New York, New York, pp. 403–418.

Wood, J.D., and P.F. Fisher, 1993. Assessing interpolation accuracy in elevation models, *IEEE Computer Graphics & Applications*, 13(2):48–56.

Wood, J.D., 1996. *The Geomorphological Characterisation of Digital Elevation Models*, Ph.D. Thesis, University of Leicester, UK, 185 p.

Yang, X., and T. Hodler, 2000. Visual and statistical comparisons of surface modeling techniques for point-based environmental data, *Cartography and Geographic Information Science*, 27(2):165–175.

Yu, Z.W., 2001. Surface interpolation from irregularly distributed points using surface splines, with Fortran program, *Computers & Geosciences*, 27(7):877–882.

(Received 11 February 2004; accepted 26 March 2004; revised 22 April 2004)